AMERICAN UNIVERSITY OF BEIRUT

OPTIMIZED OPERATION OF DISPLACEMENT VENTILATION COMBINED WITH A NOVEL EVAPORATIVE COOLED CEILING FOR A TYPICAL OFFICE IN THE CITY OF BEIRUT

by
MARIAM MOUNIR ITANI

A thesis
submitted in partial fulfillment of the requirements
for the degree of Master of Engineering
to the Department of Mechanical Engineering
of the Faculty of Engineering and Architecture
at the American University of Beirut

Beirut, Lebanon
April 2015

AMERICAN UNIVERSITY OF BEIRUT

OPTIMIZED OPERATION OF DISPLACEMENT
VENTILATION COMBINED WITH A NOVEL
EVAPORATIVE COOLED CEILING FOR A TYPICAL
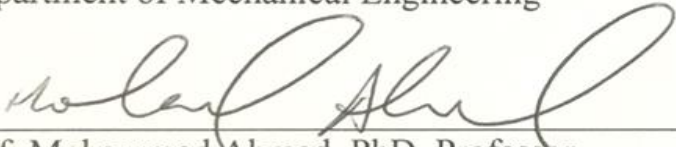OFFICE IN THE CITY OF BEIRUT

by
MARIAM MOUNIR ITANI

Approved by:

_____   Advisor
Prof. Kamel Abou Ghali, PhD, Professor
Department of Mechanical Engineering

_____   Co-Advisor
Prof. Nesreen Ghaddar PhD, Professor
Department of Mechanical Engineering

_____   Member of Committee
Prof. Mohammad Ahmad, PhD, Professor
Department of Chemical and Petroleum Engineering

Date of thesis defense: April 28, 2015

AMERICAN UNIVERSITY OF BEIRUT

THESIS, DISSERTATION, PROJECT RELEASE FORM

Student Name: _____Itani_____Mariam_____Mounir_____
                      Last   First   Middle

● Master's Thesis   ○ Master's Project   ○ Doctoral Dissertation

☑   I authorize the American University of Beirut to: (a) reproduce hard or electronic copies of my thesis, dissertation, or project; (b) include such copies in the archives and digital repositories of the University; and (c) make freely available such copies to third parties for research or educational purposes.

☐   I authorize the American University of Beirut, **three years after the date of submitting my thesis, dissertation, or project,** to: (a) reproduce hard or electronic copies of it; (b) include such copies in the archives and digital repositories of the University; and (c) make freely available such copies to third parties for research or educational purposes.

_____Mariam_____   _____6, May, 2015_____

Signature   Date

ACKNOWLEDGMENTS

AN ABSTRACT OF THE THESIS OF

<u>Mariam Mounir Itani</u>   for   <u>Master of Engineering</u>
<u>Major</u>: Applied Energy

Title: <u>Optimized Operation of Displacement Ventilation Combined with a Novel</u>
<u>Evaporative Cooled Ceiling for a Typical Office in the City of Beirut</u>

The study investigates the performance of displacement ventilation (DV) aided by a novel evaporative cooled ceiling using Maisotsenko cycle (M-cycle). The integrated DV and evaporative cooled ceiling system is known to increase the load removal of the DV air conditioning system beyond the 40 W/m2 limit with no additional energy consumption. To increase the efficiency of the evaporative cooled ceiling, solid desiccant (SD) dehumidification system regenerated by parabolic solar concentrator thermal source is used. Predictive mathematical models of the conditioned space, the SD and the evaporative cooled ceiling are integrated to study the energy performance of the suggested combined system while utilizing an optimized control strategy for typical offices of moderate humid climate. The control strategy aims to determine optimal values of supply air flow rate and temperature and regeneration temperature while meeting space load, indoor air quality, and thermal comfort requirements.

The integrated system performance is optimized to get the minimal energy cost and then compared to the cost when using a chilled ceiling displacement (CC/DV) air conditioning system.

CONTENTS

Chapter

NOMENCLATURE

δ	channel height (m)
C_p	specific heat (J/kg.K)
$\dot{q}$	radiative heat load (W/m^2)
h_{fa}	latent heat of water (J/kg)
T	temperature (∘C)
u	velocity (m/s)
w	humidity ratio (kg/kg)
w*	humidity ratio of saturated air (kg/kg)
x	position (m)
h	convective heat transfer coefficient (W/m^2.K)
h_m	mass transfer coefficient (m/s)
ρ	density (kg/m^3)
K_1	effective thermal conductivity of the heat transfer plate (W/m.K)
K_2	effective thermal conductivity of the ceiling (W/m.K)
δ_1	effective thickness of the heat transfer plate (m)
δ_2	effective thickness of the ceiling (m)
ΔT	temperature difference of air in the room and ceiling
ρ	density (kg/m^3)
K_{e1}	effective thermal conductivity of the heat transfer plate (W/m.K)
K_{e2}	effective thermal conductivity of the ceiling (W/m.K)

Subscripts

a	air
c	Ceiling
d	air in dry channel
p	heat transfer plate
r	room
1, 2	water absorbing sheets
w	working air in wet channel

ILLUSTRATIONS

TABLES

Table

CHAPTER I

COMBINED DISPLACEMENT VENTILATION NOVEL EVAPORATIVE COOLED CEILING

A. Introduction

People nowadays spend about 90% of their time in indoor spaces (U.S. Environmental Protection Agency, 1989). This means that, unless indoor air is treated and fresh air is supplied, people will spend time in an unhealthy and uncomfortable space due to long periods of exposure to pollutants. With the increasing amount of fresh air, an increase in energy consumption arises in order to condition this required fresh air. Under the fact that 60% of world-wide energy produced is spent in residential buildings (EIA), the major concern in buildings aims toward ensuring thermal comfort with good indoor air quality under minimal energy consumption.

Although there exist conventional air conditioning systems that rely on mixing fresh and return air, these systems may not maintain a healthy and comfortable indoor environment where high concentrations of pollutants are found and not enough fresh air is supplied. One of the popular air conditioning systems considered to be promising in providing both thermal comfort and air quality under low energy consumption is displacement ventilation (DV) (Jiang, Z.; Q. Chen and A. Moser, 1998) (X. Yuan; Q. Chen and L.R. Glicksman). The DV system provides the supply fresh air at low level and relies on buoyancy to drive the contaminants toward the ceiling level to be exhausted (W. Chakroun; K. Ghali and N. Ghaddar, 2011). By that, the space is divided into two regions; lower occupied fresh and cool air region and an upper contaminated

region above the breathing level of occupants (Mohamad Ayoub; Nesreen Ghaddar and Kamel Ghali, 2006) (Mossolly M.; N. Ghaddar; K. Gali and L. Jensen, 2008). To ensure thermal comfort and prevent thermal drafts at the occupied level, DV air conditioning systems supply air at temperatures not less than 18°C and velocities not more than 0.2 m/s (ASHRAE Handbook, 2009). These two restrictions impose a limitation on the ability of the DV system to remove sensible loads higher than 40 W/m^2. Such limitations have encouraged researchers to consider using chilled ceilings (CC) that aid the DV system in increasing the load removal capacity above the limit of 40 W/m^2 (A. Keblawi; N. Ghaddar; K. Ghali and L. Jensen, 2009) (S.J. Rees and P. Haves, 2001). However, a CC/DV system consumes a lot of energy to cool the ceiling and has the risk of condensation taking place on the ceiling surface when the air near it reaches the dew point temperature (X. Hao, G. Zhang, Y. Chen, S. Zou and D. J. Moschandreas, 2007) (Bahman, A.; W. Chakroun; R. Saadeh; K. Ghali and N. Ghaddar, 2008). This leads to the suggestion of a passive way to cool the ceiling without additional energy consumption by using a novel evaporative cooled ceiling (Chandrakant Wani; Satyashree Ghodke and Chaitanya Shrivastava, 2012). A study by Miyazaki et al. (Takahiko Miyazaki; Atsushi Akisawa and Isao Nikai, 2011) investigated the thermal performance of a passive cooling device represented by a dew point evaporative cooler, which uses the concept of the Maisotsenko cycle, integrated with a ceiling panel and a solar chimney. This cooler takes the air from the room and then cools down due to water evaporation after absorbing the heat from the air. Cooling air under the Maisotsenko cycle results in having an air temperature that approaches the dew point temperature, rather than approaching the wet bulb temperature which is higher for non-

saturated air (Ala Hasan, 2010) (B. Riangvilaikul and S. Kumar, 2010). Results of the study by Miyazaki et al. (Takahiko Miyazaki; Atsushi Akisawa and Isao Nikai, 2011) stated that the ceiling can remove 40-50 W/m^2 of radiative cooling load without having a considerable increase in its temperature.

The performance of the novel evaporative cooled ceiling depends on different parameters, mainly on the humidity level in the air and the velocity of air passing through the ceiling (B. Riangvilaikul and S. Kumar, 2010) (Changhong Zhan; Xudong Zhao; Stefan Smith and S.B. Riffat, 2011) (Maheshwari GP; Al-Ragom F and Suri RK, 2001). Thus, in order to make the use of evaporative cooled ceiling a viable option, dehumidification of the supply air is needed. Desiccant wheel dehumidification is used, where it utilizes the available solar energy to regenerate the desiccant (Meckler M, 1995) (Ghali K.; Othmani, M.; Ghaddar, N, 2008).

In contrary to conventional systems that rely on varying one parameter only to meet space loads, the presence of different parameters that affect the performance of the proposed system (the humidity level in the supply air and the flow rate as well as the temperature of the supply air) gives reason to search for optimal values of these parameters that enhance the system performance and minimize energy consumption as well. Optimal values of the different parameters can be found by performing optimization for the integrated system that gives the optimum energy cost of the system while maintaining thermal comfort and air quality in the space.

In this study, the different systems including the DV system aided by the novel evaporative cooled ceiling that uses no additional energy, and the solid desiccant dehumidification system that is regenerated through solar collectors utilizing the

3

renewable solar energy, will be integrated and optimized to provide comfort and good air quality in the occupied zone at minimal energy cost for an office space in the city of Beirut. The energy consumed by the optimized proposed system will be compared to that consumed under an optimized CC/DV air conditioning system.

B. System Description

The proposed integrated system applied in a hot and humid climate for space cooling is presented in Fig. 1. The hybrid air conditioning system is composed of a desiccant wheel, a sensible wheel, a cooling coil, a regenerative coil, supply and exhaust fans, parabolic solar collectors, an auxiliary heater and an evaporative cooled ceiling. Initially, the fresh air fan draws outside air and passes it through a desiccant dehumidification wheel for dehumidification which will result in an increase in the air temperature. Then, the air stream is cooled by exchanging heat with the exhaust air through the use of a sensible wheel. After that, the air is further cooled by the cooling coil to the desired supply temperature and supplied to the space. Cool supply air enters the space at floor level and removes the load from the space as it rises toward the ceiling due to buoyancy forces. Consequently, the bottom occupied zone contains the fresh cool air, while the heat present in the space due to internal and external loads rises to the ceiling level. Before leaving the space, the return air will pass through a ceiling dry channel followed by another wet channel to lower the temperature of the ceiling. The return air is then used after heating it for regenerating the desiccant. Finally, the humid air is exhausted to the atmosphere. It is noted that the heat input needs of the

4

regeneration coil are provided partly by parabolic solar concentrators and by an auxiliary heater.
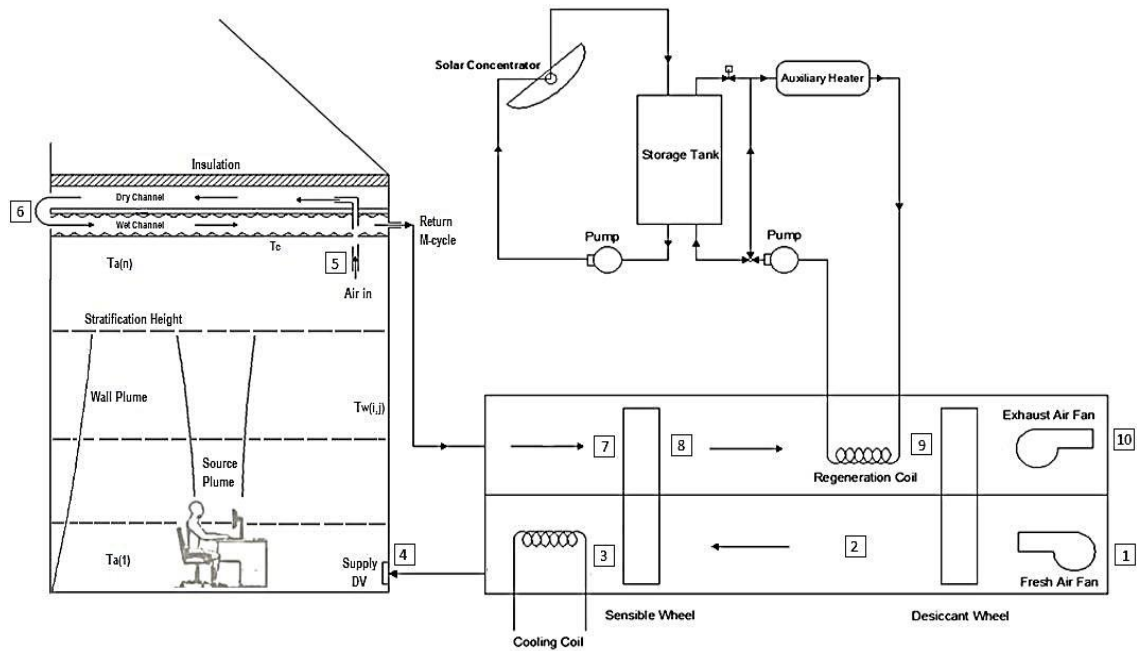
Figure 1: Schematic of the combined air conditioning system

C. Modeling Methodology

In order to study the performance of the above described system, mathematical models for different system components shall be developed and integrated to formulate the optimization problem. These models include the solar concentrator storage tank with the regeneration coil models and the desiccant wheel with the different heat exchanger models that are used to get the space supply air conditions at each hour of system operation. Then, a DV space cooling model with the evaporative cooled ceiling model are integrated to find the cooling load of the system and the conditions of the space including the vertical temperature distribution and the stratification height.

After integrating and solving the different system models, the energy consumed by the different system components (supply and exhaust fans, auxiliary heater and cooling coil) is calculated and minimized to give the minimum possible cost during each hour of system operation. Genetic algorithm is a tool used for optimization and is efficient for optimizing a system of multi-models that are integrated and undergo some constraints to get the minimum objective cost function (Mitchell, M., 1997). The energy consumption is minimized while having thermal comfort and good air quality in the space. The genetic algorithm optimizer will search for the optimal values of the following variables:

- Regeneration temperature

- Space supply air flow rate

- Space supply air temperature

CHAPTER II

INTEGRATION OF THE PROPOSED SYSTEM WITH THE DESICCANT AND SOLAR CONCENTRATOR STORAGE TANK MODELS

To predict the system's performance, mathematical models for different system components are introduced as follows:

A. Displacement Ventilation Space Model

A space model will be needed to evaluate the system's performance. The space model should be capable of predicting the indoor air temperature for given internal loads, outdoor ambient conditions and building envelope material. The physical model of the DV plume-multi-layer thermal space of Ayoub et al. (K. Ghali; N. Ghaddar and M. Ayoub, 2007) is adopted. The model assumes air movement in the vertical direction dividing the space into several horizontal layers as shown in Fig. 1. In each layer, the model takes into account the different flow rates for the wall plume, heat source plume, and the surrounding air on the upper and lower sides of the air layer. The building envelope consists of walls with multi layers divided into a number of nodes to model the temperature distribution along the wall layers. The wall model with the wall and source plume models were integrated to predict the stratification height in the space and the vertical distribution of the internal air temperatures, as a function of the ceiling temperature predicted from the evaporative cooled ceiling model and space air supply conditions.

B. Evaporative Cooled Ceiling Model

As shown in Fig. 2, the upper space warm air is directed to pass through a dry channel to decrease its temperature without adding any humidity to the air, and then reversing its flow to pass through a wet channel (H. Caliskan; A. Hepbasli; I. Dincer and V. Maisotsenko , 2011) (M. Itani; K. Ghali and N. Ghaddar, 2015). To predict the air temperature variation and ceiling temperature, different energy equations are used for both channels using the development of Miyazaki et al. (Takahiko Miyazaki; Atsushi Akisawa and Isao Nikai, 2011) assuming that the heat transfer by conduction within the heat transfer plate, the water sheets and the ceiling is negligible, as well as that the heat gain through the roof is neglected as the top side of the dry channel is insulated.
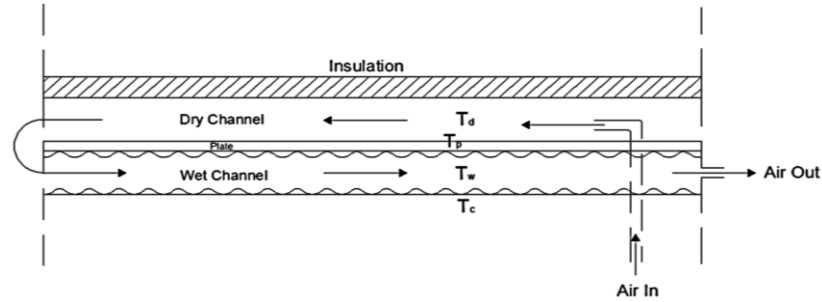
Figure 2: Schematic of the Ceiling Setup

Energy balance for the air in the dry and wet channels

$$\{\rho C_p u \delta / h\}_d (dT_d / dx) = (T_p - T_d) \tag{1}$$

$$\{\rho C_p u \delta\}_w (dT_w / dx) = h_1 (T_1 - T_w) + h_2 (T_2 - T_w) \tag{2}$$

The right term of Eq. (1) and Eq. (2) represent the net convective heat flow in the dry and wet channels respectively. The terms h_d and h_w represent the convective heat transfer coefficients in the dry and wet channels and δ_d and δ_w represent the

8

channel heights of both dry and wet channels. The left hand side of Eq. (1) represents the heat exchange in the dry channel, while the left hand side of Eq. (2) represents the heat exchange with the two sides of the wet channel.

Energy balance of the two water sheets

$$h_1(T_w - T_1) + \rho_d h_{m1} h_{fg}(w - w^*) = (\frac{K_1}{\delta_1})(T_1 - T_p) \tag{3}$$

$$h_2(T_w - T_2) + \rho_d h_{m2} h_{fg}(w - w^*) = (\frac{K_2}{\delta_2})(T_2 - T_c) \tag{4}$$

In Eq. (3), the upper water sheet exchanges heat with the plate and exchanges sensible and latent heat transfer with the flowing air. Similarly, in Eq. (4) the lower water sheet exchanges conduction heat transfer with the ceiling plate and sensible and latent heat with the flowing air. The terms T_1 and T_2 represent the temperatures of the two water sheets in the wet channel. T_c is the chilled ceiling temperature and the h_{fg} is the latent heat of vaporization. The term w^* represents the humidity ratio of saturated air at temperature T_w, and h_{m1} and h_{m2} represent the convective mass transfer coefficients with the two sides of the wet channel.

Mass balance of the air in the wet channel

$$dw / dx = [(h_{m2} + h_{m2}) / \{u\delta\}_w](w^* - w) \tag{5}$$

The right hand side of Eq. (5) represents the net convective flow of moisture in the wet channel and the left hand side represents the moisture exchanges with the two water sheets of the wet channel.

Energy balance for the plate separating the wet and dry channels

$$h_d(T_d - T_p) + (\frac{K_1}{\delta_1})(T_1 - T_p) = 0 \qquad (6)$$

The first left term in Eq. (6) represents the heat transfer with the dry air and the second term represents the conductive heat flow with the water sheet, where K_1 and δ_1 represent the effective plate thermal conductivity and plate thickness respectively.

Energy balance of the ceiling

$$(\frac{K_2}{\delta_2})(T_2 - T_c) + h_r(T_r - T_c) + \dot{q} = 0 \qquad (7)$$

The ceiling exchanges heat with the water sheet of the wet channel in Eq. (7) as well as convective and radiative heat transfer with the space. The terms K_2 and δ_2 represent the effective ceiling plate thermal conductivity and ceiling thickness respectively.

C. Desiccant Model

The products offered by. The desiccant machine consists of a rotary wheel divided into two sections for two counter-flow air passages. In one passage, the hot dry air regenerates the desiccant and is then exhausted to the outside, and in the other passage, the air is dehumidified before being cooled and injected into the cooled space. For the desiccant wheel, the model developed by Beccali et al. (M.Beccali; R.S. Adhikari; F. Butera and V. Franzitta. , 2004) and used by Hourani et al. (M. Hourani; K. Ghali and N. Ghaddar, 2014), will be implemented. This simple model offers the added option of calculating the air characteristics (enthalpy and relative humidity) even when

the volume air flow ratio between supply and regeneration side differs from one.

However, the range of variation of the different model parameters is as follows:

- Regeneration temperature between 40°C and 80°C.

- Regeneration air humidity ratio between 10 g/Kg and 16 g/Kg.

- Inlet air temperature between 20°C and 34°C.

- Inlet air humidity ratio between 8 g/Kg and 15 g/Kg.

D. Solar Concentrator Storage Tank Model

In order to utilize the available solar radiation, parabolic solar concentrators are used to provide hot water for heating the air that regenerates the solid desiccant. The model developed by Duffie and Beckman (Duffie J and Beckman W, 2003) is used to estimate the useful heat gain by the antifreeze solution flowing in the solar collector. This heat gain depends on the aperture and receiver area of the collector, the heat removal factor and heat transfer loss coefficient of the collector, the temperature of the antifreeze solution that flows in the collector and the temperature of ambient air. The model is also used to find the transient water temperature in the hot water storage tank. The transient water temperature depends on the volume and surface area of the tank, the heat lost from the tank, the useful heat gained by the solar collector and the ambient air temperature.

E. Optimization Tool

The variables that are used by the genetic algorithm optimizer to reach minimum energy consumption in this study are the regeneration temperature, supply air

11

flow rate and supply air temperature. The objective function *I* representing the
operational cost of the system for a given time is as follows:

$$I = \alpha_f J_{fans} + \alpha_h J_{heater} + \alpha_c J_{cooling} + \alpha_H J'_H + \alpha_{gt} J'_{gt} + \alpha_{PPD} J'_{PPD} \tag{8}$$

Where J_{fans}, J_{heater}, $J_{cooling}$, J'_H, J'_{gt} and J'_{PPD} represent the fan energy cost (W),
the auxiliary heater energy cost (W), the cooling coil energy cost (W), the stratification
height constraint, the temperature gradient constraint and the percent people dissatisfied
constraint, respectively.

The stratification height constraint term J'_H represents the normalized
deviation from the minimum stratification height set by the constraints and is given as:

$$J'_H = \exp(\frac{H_{min}}{H}) - 1 \tag{9}$$

The exponential term helps to penalize the cost function each time the
stratification height in the room *H* decreases below the minimum set value H_{min}. This
will increase the value of the cost function radically and the set of variables at hand is
rejected (A. Keblawi; N. Ghaddar and K. Ghali , 2011) (M. Hammoud; K. Ghali and N.
Ghaddar, 2014).

Similarly, Eq. (10) and Eq. (11) permit taking into consideration the maximum
allowed temperature gradient and percent people dissatisfied, respectively, to find their
corresponding cost.

$$J'_{gt} = \exp(\frac{gt}{gt_{max}}) - 1 \tag{10}$$

$$J'_{PPD} = \exp(\frac{PPD}{PPD_{max}}) - 1 \tag{11}$$

The coefficients α_f, α_h, α_c α_H, α_{gt} and α_{PPD} represent the fans weighing factor ($/W), the auxiliary heater weighing factor ($/W), the cooling coil weighing factor ($/W), the stratification height weighing factor ($), the temperature gradient weighing factor ($) and the percent people dissatisfied weighing factor ($), respectively.

The constraints that are set on the system are:

- Temperature gradient in the occupied zone < 2.5 °C/m

- Stratification height > 1.1 m

- Percent People Dissatisfied $<10\%$

F. Solution Methodology

The sequence of operation of the integrated system is represented by the flow chart in Fig. 3. The genetic algorithm optimizer selects values for the different variables; regeneration temperature, supply air flow rate and temperature. The selected variables, the outdoor weather conditions (Solar radiation, ambient conditions, etc.), the space dimensions and the internal heat loads are required as inputs to the different system models.

The solar concentrator storage tank with the regeneration coil models are used to get the regenerated air conditions and the energy consumed for regeneration, where the regenerated air is then cooled and supplied to the space. The space model finds the internal surface temperatures and the load subjected to the ceiling in order for the ceiling model to find the ceiling temperature. Then, the updated temperatures are used to solve for the energy balance of each air layer. The coupled mass and energy equations are discretized into algebraic equations using the finite volume method. Once

13

convergence, set to 10^{-6}, is reached the temperature distribution in the space is determined as well as the energy performance of the system. Then, the optimizer will check if the system under the selected variable values meets the constraints of thermal comfort and good air quality. After that, the objective cost function is calculated and the whole procedure, from selecting variable values till finding the cost function, is repeated until the optimal values of the variables are found that give the minimum cost function while meeting indoor air quality and thermal comfort.
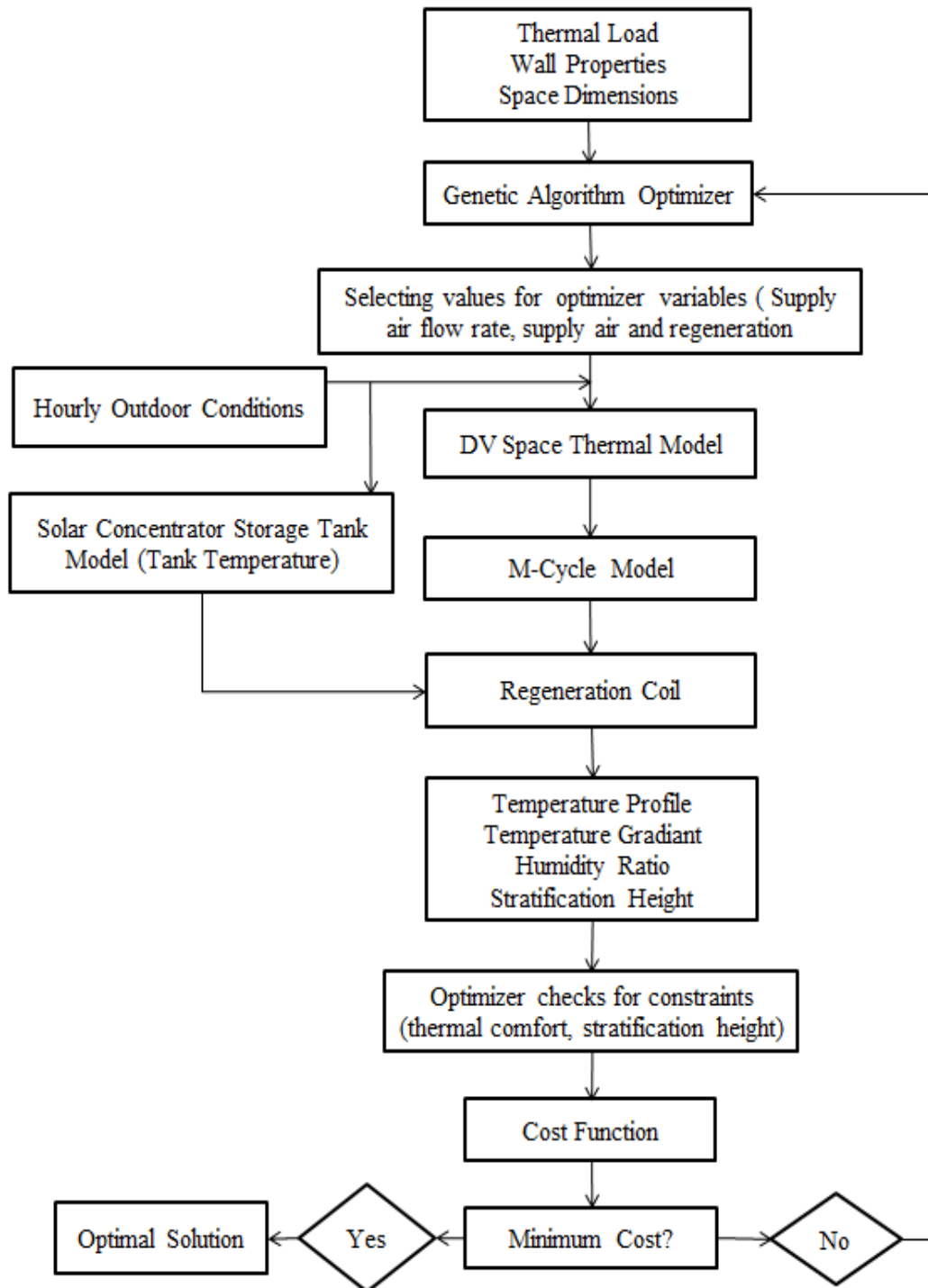
Figure 3: Flowchart showing the sequence of operation

CHAPTER III

EXPERIMENTAL VALIDATION OF DV/EVAPORATIVE COOLED CEILING

The validation of the integrated evaporative cooled ceiling and displacement ventilation model is carried out in this study to validate the air temperatures predicted at different heights in the space as well as the ceiling and different walls temperature and the sensible load that can be removed by the integrated system.

A. Experimental Setup and Measurements

Experiments were carried out in a climatic chamber, shown in Fig. 4, consisting of the displacement ventilation and evaporative cooled ceiling system, where a supply grill is located on the east wall at floor level and an exhaust grill is connected to the outlet of the ceiling setup as shown in Fig. 5(a) and Fig. 6. The chamber has a floor area of 5.56 m^2 and a height of 2.8 m, where all the walls are insulated so as to prevent the effect of solar radiation.
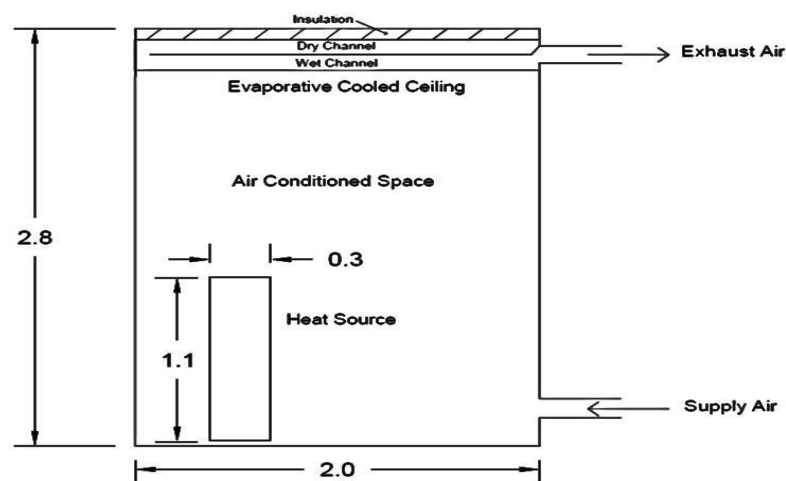
Figure 4: Schematic of Experimental Chamber

16

Figure 5: (a) Ceiling and Chamber of the Experimental Setup; (b) A Metallic Cylinder and Data Logger

Figure 6: Exhaust Grill Connected to the Ceiling of the Experimental Setup

The temperatures of the air in the chamber were measured at different heights (0.5 m, 1.1 m and 2 m), at the supply grill level and at the inlet to the ceiling setup level using OM-EL-USB-2 sensors. These sensors have an accuracy of ±0.5°C in reading the temperatures. The temperature of the ceiling and the different walls were measured using K-type thermocouples connected to OM-DAQPRO-3500 data logger set to take a reading at every minute.

The supply fan delivers air at a fixed flow rate of 0.118m^3/s and the experiment was done at a fixed temperature and relative humidity of 21°C and 50%, respectively.

The sensible load in the chamber was set at 300 W using three metallic cylinders of 0.3m diameter and 1.1m height, each equipped with a 100 W heat source, as shown in Fig. 5(b). The experiment was carried out for the displacement ventilation system operating without the evaporative cooled ceiling and then followed by the integration of the ceiling setup, so that validation can be done to both the DV system and the integrated one after reaching quasi-steady state conditions.

B. Model Validation Results

The experimental and simulation results predicted by the DV model and by the integrated DV/evaporative cooled ceiling model for the room air temperatures at different heights and for the ceiling and average wall temperatures are shown in Table 1. In regard to the DV system results, the vertical temperature variation shows an increasing trend toward the ceiling level and was 23.24°C at the height of 1.1m representing the occupied level. The ceiling temperature measured was 23.87°C and the average wall temperature was 23.83°C. The measured results showed good agreement with the model predicted values. In regard to the integrated system results, the room air temperatures measured had lower values than that of the DV system and the temperature at 1.1m was 23.02°C. The trend in the vertical temperature variation was different from the DV system and showed a decrease in the room temperature above the height of 2m due to the cooled ceiling that has a temperature of 20.7°C. It is noticed also that good agreement is found between the measured and predicted values under the integrated system.

18

Table 1: Experimental and Model Predicted Values

	DV Experiment	DV Simulation	Integrated Experiment	Integrated Simulation
$T_{\text{room at 0.5m}}$ (°C)	22.7	21.4	22.33	21.24
$T_{\text{room at 1.1m}}$ (°C)	23.24	22.05	23.02	21.97
$T_{\text{room at 2m}}$ (°C)	23.91	22.82	23.34	22.3
$T_{\text{ceiling inlet}}$ (°C)	24.55	23.49	23.05	21.96
T_{ceiling} (°C)	23.87	22.7	20.7	19.07
$T_{\text{wall avg.}}$ (°C)	23.83	22.6	23.24	21.88

CHAPTER IV

CASE STUDY

A. Case Study Description

The proposed optimization procedure for the integrated novel evaporative cooled ceiling and DV systems is applied to a case study represented by an office space located in Beirut. The electric power consumption of the optimized system is then calculated and compared to that of the CC/DV system resulting with the same chilled ceiling temperature for every hour of operation.

The case study considered is an office that has a 6m x 5m floor dimensions and a height of 2.8m. It consists of one exposed wall on the south façade and the remaining walls along with the floor are partitioned with conditioned spaces. The walls are assumed to have the same construction with an overall heat transfer coefficient of 2.36 W/m^{2}K and divided into 17 discrete nodes of 0.01m spacing. The internal sensible and latent load schedules for a typical day in the office are shown in Table 2. The maximum number of space occupants is 6 and the space is occupied from 7 a.m. till 7 p.m., where the maximum latent load due to moisture generation from occupants is 300 W. The total sensible load that the system should remove includes not only the internal one but also the external load that reaches a peak of 61 W/m^2, which is greater than the ability of the DV system to remove unaided. The parabolic solar concentrator is selected to have a length of 2.4m and a width of 1.2m. More specifications for the solar concentrator are shown in Table 3. Two solar concentrators are used and connected to a hot water

storage tank having a volume of 0.4m^3 and an auxiliary heater to provide the heat

needed for regenerating the solid desiccant. The solar concentrators and storage tank

occupy not more than 25% of the roof area and are selected to provide a high solar

fraction value in order to gain as much heat as possible from the solar radiation incident

on the solar concentrators.

Table 2: Hourly outdoor weather conditions for the month of July and internal sensible
and latent loads

Hour	Dry Bulb Temperature (°C)	Horizontal Surface Radiation (W.hr/m²)	Humidity ratio (Kg/Kg)	Internal Sensible Load (Watt)	Internal Latent Load (Watt)
1	24.3	0	0.01222	0	0
2	23.9	0	0.01199	0	0
3	23.5	0	0.01177	0	0
4	23.2	0	0.01164	0	0
5	22.9	0	0.01139	0	0
6	22.8	30.73	0.01143	0	0
7	23.1	86.31	0.01156	500	100
8	23.8	156.38	0.01204	500	100
9	25.1	231.84	0.01255	500	100
10	26.4	300.79	0.01338	750	150
11	27.8	351.33	0.01422	750	150
12	28.8	374.78	0.01483	1000	200
13	29.7	366.03	0.01537	1500	300
14	30.2	328.02	0.01578	1500	300
15	30.5	266.28	0.01596	1500	300
16	30.4	192.64	0.01601	750	150
17	30	118.58	0.01555	750	150
18	29.2	55.02	0.01512	500	100
19	28.2	3.64	0.01449	500	100
20	27.2	0	0.01389	0	0
21	26.4	0	0.01338	0	0
22	25.8	0	0.01308	0	0
23	25.2	0	0.01278	0	0
24	24.7	0	0.01245	0	0

Table 3: Parabolic solar concentrator specifications

Parameter	Value
Length	2.4 m
Width	1.2 m
Receiver emittance	0.3
Absorber diameter	0.06 m
Transparent envelope outer diameter	0.09 m
Thickness of transparent envelope	0.004 m
Thermal conductivity of tube	16 W/m °C
Wall thickness of tube	0.05 m
Specific heat of fluid in collector (water)	4186 J/Kg °C

Optimizing the operation of the integrated system will start from the first occupied hour (7 a.m.) till the last occupied one (7 p.m.). The genetic algorithm optimizer will set values for the supply air flow rate and temperature and regeneration temperature. Then it will find the corresponding energy cost under these values and checks for the constraints of thermal comfort and air quality during each hour of occupation. This step will be repeated until the optimizer finds the set of variables that meet the constraints with the minimal possible energy cost. During unoccupied hours, cooling and dehumidification of the supply air are not applied; however, simulation is done in order to get the initial space temperatures, the humidity levels, and storage tank temperature conditions. The searching range for the optimal supply air flow rate value is between 0.1 and 0.3 m³/s, for the optimal supply air temperature is between 18 and 24 °C and optimal regeneration temperature between 40 and 80 °C. Simulation for the system is done for the whole cooling season represented by five months, from June to October, where the 21st of each month is taken as representative of that month.

The outdoor setup made up of the solid desiccant dehumidification system and the cooling coil will be common for the proposed and the CC/DV system. The chilled ceiling in the CC/DV system will be modeled as a constant temperature that could be varied hourly throughout the day. The supply air flow rate and temperature can be also varied to calculate the corresponding electric power consumption by the different system components (fans, auxiliary heater and chiller). The electric power consumed by the supply and exhaust fans (P_{fan}) can be calculated as follows:

$$P_{fan} = \frac{Q \times \Delta P}{\eta_{fan}} \tag{12}$$

Where Q is the fan volumetric flow rate, ΔP is the pressure rise in the fan and η_{fan} is the fan efficiency equivalent to 80% as typical for such applications. The auxiliary heater electric power consumption is estimated to be the same as its thermal energy consumption, so having an efficiency of 100%. Finally, the electric power consumed by the chiller ($P_{chiller}$) is calculated as follows:

$$P_{chiller} = \frac{E_{chiller}}{COP} \tag{13}$$

where $E_{chiller}$ is the thermal energy consumed by the chiller and COP is the coefficient of performance of the chiller with a value of 3.5.

B. Results and Discussion

After performing optimization for the case study, hourly results of the total energy consumed are obtained. In order to assess the performance of the proposed

system incorporating a novel evaporative cooled ceiling/DV air conditioning system, a comparison will be done between the total electric power consumed on the simulated day under this system and the total electric power consumed on the simulated day under a CC/DV air conditioning system. In order for the comparison to be valid, a similar level of thermal comfort and air quality should be attained by the two systems.

During the month of July, following the load profiles shown in Table 2 and following the transient outdoor conditions, the proposed system optimization results showed changes at every hour of system operation for the supply air flow rate and temperature and regeneration temperature. These optimized values will provide the necessary amount for space cooling while meeting the constraints of thermal comfort and air quality at minimum cost of operation.

Table 4: The hourly optimal values of supply flow rate and temperature and regeneration temperature,the load removed by the DV, the total load removed by the system, the energy used by the auxiliary heater and the electrical power consumed by the proposed system for the month of July

Hour	Q_{supply} (m^3/s)	T_{supply} $(°C)$	T_{reg} $(°C)$	$T_{ceiling}$ $(°C)$	DV Load Removal (W/m^2)	Total Load Removal (W/m^2)	Auxiliary Energy (KWh)	Electrical Power (KWh)
7	0.1	22.48	52	20.54	11.78	19.4	0	0.382
8	0.105	22.4	54	20	11.93	18.6	0	0.4
9	0.11	21.97	55	20.62	12.96	17.18	0	0.532
10	0.12	21.74	56.37	20.02	16.94	28.6	0	0.728
11	0.12	21.35	56.8	20.75	18.84	27.6	0	0.763
12	0.136	20.67	60.5	20.28	20.81	34.36	0.066	0.824
13	0.17	19.76	62.27	20.73	38.07	50.96	0.069	1.4
14	0.16	18.83	63.24	20.52	38.87	50.82	0.103	1.566
15	0.15	18.38	62.35	20.53	40.77	51.5	0.092	1.4
16	0.11	21.24	58.54	20.51	13.23	25.24	0.046	0.844
17	0.11	21.20	57.94	20.34	20.18	26	0.024	0.8
18	0.106	21.14	56.95	20.44	11.2	17.3	0	0.743
19	0.1	22.38	55	20	10.9	17.15	0	0.59

Table 4 shows the hourly optimal values of the supply air flow rate and temperature and regeneration temperature as well as the ceiling temperature. It also shows the simulation results of the hourly load removed by the DV, the total load removed by the system and the optimized electrical consumption of the auxiliary heater, fans and cooling coil. During the early hours of operation, hours 7 to 9, both sensible and latent loads are low and the outdoor temperature and humidity ratio are relatively low (23.1 to 26.4°C and 11.56 to 12.55 g/Kg). The optimizer selected low values of supply flow rate and high values of supply air temperature to meet the corresponding sensible load in the space. The optimizer also selected low values of regeneration temperature resulting in no electric consumption by the auxiliary heater, since the available solar energy and the lower outdoor humidity ratio made the solar collectors provide sufficient heat to regenerate the desiccant. In the following hours, hours 10 to 15, both sensible and latent loads reached their peaks and the outdoor temperature and humidity ratio reached their highest values of 30.5°C and 16.01 g/Kg, respectively. The optimizer showed an increasing trend in the supply flow rate and a decreasing one in the supply temperature, allowing the system to remove the higher sensible loads, and it showed an increasing trend in the regeneration temperature to remove the higher latent load in the space. As a result, the electric power consumption had an increasing trend due to the additional fan power and additional cooling to low supply temperatures. Also, the available solar energy was not enough to increase the storage tank temperature and provide the system with the higher regeneration temperature so the power consumed by the auxiliary heater increased. After hour 15, the occupancy level decreased, reducing

25

the internal sensible and latent loads, and the outdoor temperature and humidity ratio decreased as well. In response to the previous changes, the optimizer selected lower values of supply flow rate, higher values of supply temperature and lower values of regeneration temperature to remove the lower loads in the space. Thus, the electric power consumption of the system had a decreasing trend in the late hours of operation. It is noted that during all hours of operation, thermal comfort and good air quality measures (Stratification height, temperature gradient and percent people dissatisfied) were satisfying the requirements. The trend for the ceiling temperature was noticed to be almost constant throughout the hours of operation and having an average value of 20.38 ºC. This implies that the optimizer selected the variables that allow removing the additional sensible and latent load from the space during peak loads without having a decrease in the performance of the ceiling.
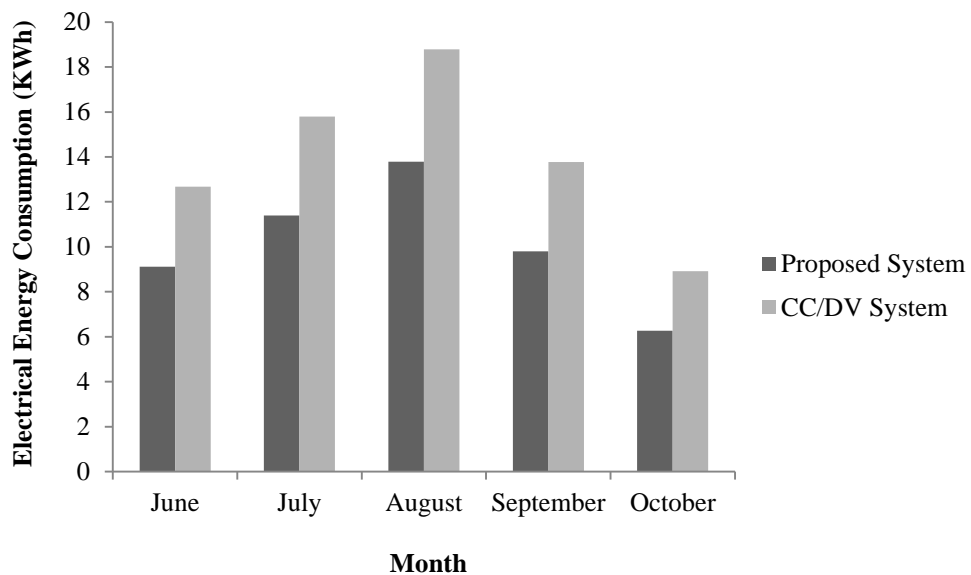

Figure 7: Electrical Energy Consumption for the Proposed and CC/DV Systems in the Different Months of the Cooling Season

26

Fig. 7 shows the total electrical energy consumption of both the proposed and the CC/DV system during the different months of the cooling season. The maximum electric energy consumed was observed during the month of August. Higher values of electric power consumption are observed in the CC/DV system, mainly due to more cooling needed to supply the chilled ceiling with cool water. The total electrical energy consumed by the proposed system during the cooling season was 50.3 KWh and that consumed by the CC/DV system was 70 KWh. Thus, a 28.14% reduction in total electric energy consumption was attained when using the proposed system.

In order to assess whether the proposed system should be considered for investment over the CC/DV system, a life cycle cost assessment is performed. The assessment takes into consideration the initial cost of the evaporative cooled ceiling and the initial cost of the chilled ceiling panels. It also considers the operating electric energy cost of the two systems over their life spans, 20 years, assuming they have no salvage value. The cost of the evaporative cooled ceiling for the case study was at 80 $/m^2, so with an area of 30 m^2 the initial cost of the ceiling is $2400. The cost of installing chilled ceiling panels is taken to be 36 $/m^2, so with an area equivalent to 30 m^2 the initial cost of the panels is $1080. On the other hand, the CC/DV system requires cooled water to enter the chilled ceiling panels and therefore, it requires a higher chiller size to provide the cooled water needed. The additional cooling required by the CC/DV system was estimated to be 2.8 KW, resulting with $900 as incremental initial chiller cost. The initial cost of using the proposed system is thus $420 more than the CC/DV system. The electric cost in Beirut City is estimated at 0.15 $/KWh and the discount rate at 3%. The operation cost over a period of 5 months of cooling per year for the

proposed system is $227, whereas that of the CC/DV system is $315, so the savings per year when using the proposed system is $88. Thus, a discounted payback period equivalent to 5 years and 2 months is attained when implementing the proposed system in this study.

C. Conclusion

A genetic algorithm optimization procedure for a combined displacement ventilation novel evaporative cooled ceiling system is developed in order to enhance cooling by the DV system with minimum energy consumption. The procedure ensures meeting the constraints of thermal comfort and good indoor air quality in spaces. The optimized system is applied to a typical office space in Beirut where its electric power consumption is compared with that of a CC/DV system resulting in the same thermal comfort level. The use of the proposed system was shown to be viable and cost effective with a payback period equivalent to 5 years and 2 months.

BIBLIOGRAPHY

Retrieved May 2, 2015, from http://www.eia.gov/forecasts/aeo

A. Keblawi; N. Ghaddar and K. Ghali . (2011). Model-based optimal supervisory control of chilled ceiling displacement ventilation system. *Energy and Buildings, 43*, 1359–1370.

A. Keblawi; N. Ghaddar; K. Ghali and L. Jensen. (2009). Chilled ceiling displacement ventilation design charts correlations to employ in optimized system operation for feasible load ranges. *Energy and Buildings, 41*(11), 1155-1164.

Ala Hasan. (2010, November). Indirect Evaporative Cooling of Air to a Sub-Wet Bulb Temperature. *Applied Thermal Engineering, 30*(16), 2460-2468.

ASHRAE Handbook. (2009). Fundamentals Chapter 9. Atlanta: American Society of Heating Refrigerating and Air-Conditioning Engineers.

B. Riangvilaikul and S. Kumar. (2010). An Experimental Study of a Novel Dew Point Evaporative Cooling System. *Energy and Buildings, 42*, 637-644.

B. Riangvilaikul and S. Kumar. (2010). Numerical study of a novel dew point evaporative cooling system. *Energy and Buildings, 42*, 2241-2250.

Bahman, A.; W. Chakroun; R. Saadeh; K. Ghali and N. Ghaddar. (2008). Performance Comparison Conventional and Chilled Ceiling/Displacement Ventilation Systems in Kuwait. *ASHRAE Transactions, 115*(1), 587-94.

Chandrakant Wani; Satyashree Ghodke and Chaitanya Shrivastava. (2012). A Review on Potential of Maisotsenko Cycle in Energy Saving Applications Using Evaporative Cooling. *International Journal of Advance Research in Science, Engineering and Technology, 1*(1), 15-20.

Changhong Zhan; Xudong Zhao; Stefan Smith and S.B. Riffat. (2011). Numerical study of a M-cycle cross-flow heat exchanger for indirect evaporative cooling. *Building and Environment, 46*, 657-668.

Duffie J and Beckman W. (2003). *Solar engineering of Thermal Processes, 3rd ed. .* John Wiley & Sons, INC.

Ghali K.; Othmani, M.; Ghaddar, N. (2008). Energy Consumption and Feasibility Study of a Hybrid Desiccant Dehumidification Air Conditioning System in Beirut. *International Journal of Green Energy, 5*(5), 360-372.

H. Caliskan; A. Hepbasli; I. Dincer and V. Maisotsenko . (2011). Thermodynamic performance assessment of a novel air cooling cycle: Maisotsenko cycle. *International Journal of Refrigeration, 34* , 980–990.

Jiang, Z.; Q. Chen and A. Moser. (1998). Indoor Airflow with Cooling and Radiative/Convective Heat Source. *ASHRAE Transactions, 98*, 33-42.

K. Ghali; N. Ghaddar and M. Ayoub. (2007). Chilled ceiling and displacement ventilation system: An opportunity for energy saving in Beirut. *International Journal of Energy Research, 31*, 743-759.

M. Hammoud; K. Ghali and N. Ghaddar. (2014). The Optimized Operation of a Solar Hybrid Desiccant/Displacement Ventilation Combined with a Personalized Evaporative Cooler. *International Journal of Green Energy, 11*(2), 141-160.

M. Hourani; K. Ghali and N. Ghaddar. (2014). Effective desiccant dehumidification system with two-stage evaporative cooling for hot and humid climates. *Energy and Buildings, 68*, 329–338.

M. Itani; K. Ghali and N. Ghaddar. (2015). Performance evaluation of displacement ventilation system combined with a novel evaporative cooled ceiling for a typical office in the city of Beirut. *7th International Conference on Applied Energy.* Abu Dhabi.

M.Beccali; R.S. Adhikari; F. Butera and V. Franzitta. . (2004). Update on desiccant wheel system. *International Journal of Energy Research, 28*, 1043–1049.

Maheshwari GP; Al-Ragom F and Suri RK. (2001). Energy saving potential of an indirect evaporative cooler. *Applied Energy*, 69-76.

Meckler M. (1995). Desiccant Outdoor Air Pre-Conditioners Maximize Heat Recovery Ventilation Potentials. *ASHRAE Transactions Symposia*, SD-95-9-4.

Mitchell, M. (1997). *An Introduction to Genetic Algorithm.* London: The MIT Press.

Mohamad Ayoub; Nesreen Ghaddar and Kamel Ghali. (2006). Simplified Thermal Model of Spaces Cooled with Combined Displacement Ventilation and Chilled Ceiling System. *ASHRAE International Journal of HVAC&R Research, 12*(4), 1005-1030.

Mossolly M.; N. Ghaddar; K. Gali and L. Jensen. (2008). Optimized Operation of Combined Chilled Ceiling Displacement Ventilation System Using Genetic Algorithm. *ASHRAE Transactions*, SL-08-055.

S.J. Rees and P. Haves. (2001). A Nodal Model for Displacement Ventilation and Chilled Ceiling sSystems in Office Spaces. *Building and Environment, 36*(6), 753-762.

Takahiko Miyazaki; Atsushi Akisawa and Isao Nikai. (2011, September). The cooling performance of a building integrated evaporative cooling system driven by solar energy. *Energy and Buildings, 43*(9), 2211-2218.

U.S. Environmental Protection Agency. (1989). *Report to Congress on Indoor Air Quality: Volume 2.* Washington, DC.

W. Chakroun; K. Ghali and N. Ghaddar. (2011). Air Quality in Rooms Conditioned by Chilled Ceiling and Mixed Displacement Ventilation for Energy Saving. *Energy and Buildings, 43*, 2684-2695.

X. Hao, G. Zhang, Y. Chen, S. Zou and D. J. Moschandreas. (2007). A Combined System of Chilled Ceiling, Displacement Ventilation and Desiccant Dehumidification. *42*, 3298-3308.

X. Yuan; Q. Chen and L.R. Glicksman. (1998). A Critical Review of Displacement Ventilation. *Energy and Buildings, ASHRAE Transactions, 104*, 78-90.